Maxwell's demon and Feynman's ratchet

I Maxwell's demon

II Feynman's ratchet

III Molecular motors

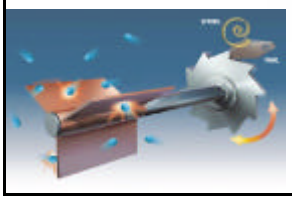

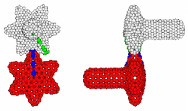

James Clerk Maxwell (1831-1879)

Maxwell's demon

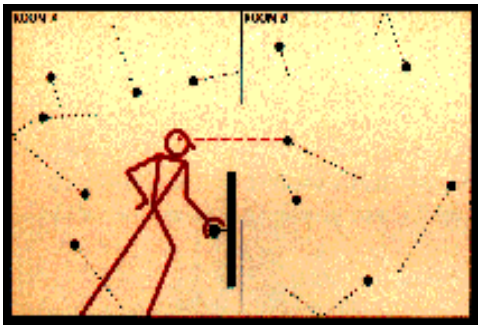

Richard Phillips Feynman (1918-1988)

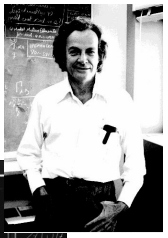

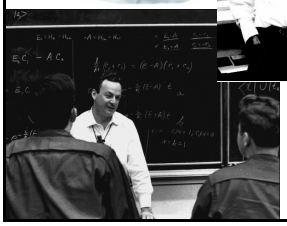

http://www.caltech.edu/cgi-bin/arcquery?Feynman

Physics of ratchets

pawl

asymetric tooths

The Feynman Lectures on Physics, I-46

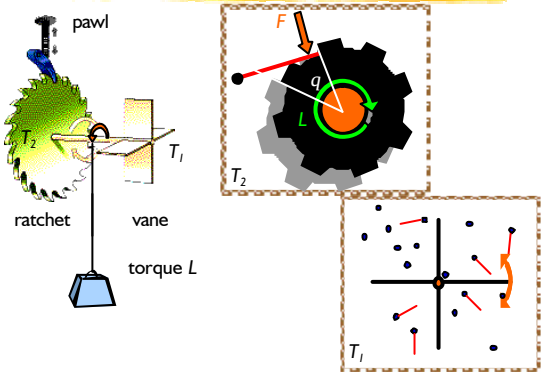

Forward rotation

e	energy to lift the pawl
Lq	work done on load
$e+Lq$	energy to rotate wheel by one tooth
$f_B^f = Z^{-1}e^{-(e+Lq)/t_1}$	Boltzmann factor for work provided by vane
$n\, f_B^f$	ratching rate with n attempt frequency
$n\, f_B^f Lq$	power delivered

e energy provided to ratchet

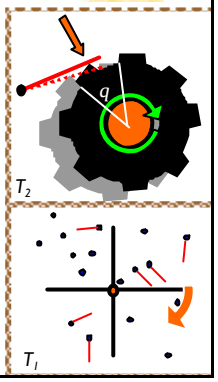

Backward rotation

e	energy to lift the pawl
Lq	work provided by load
$e+Lq$	energy given to vane
$f_B^b = Z^{-1}e^{-e/t_2}$	Boltzmann factor for tooth slip
$n\, f_B^b$	slip rate with attempt frequency n

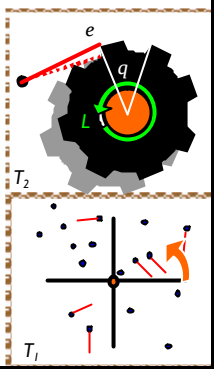

Equilibrium and reversibility

ratching rate = slip rate $f_B^b = f_B^f$

$$L_{eq}q = \left(\frac{t_1}{t_2} - 1\right)e$$

Reversible process by increasing the load infinitesimally from equilibrium L_{eq}. This forces a rotation leading to heating of reservoir 1 with $dq_1 = e + L_{eq}$? and cooling of reservoir 2 as $dq_2 = -e$:

$$\frac{dq_1}{-dq_2} = \frac{e + L_{eq}q}{e} = \frac{t_1}{t_2}$$

$$\frac{dq_1}{t_1} + \frac{dq_2}{t_2} = dS_1 + dS_2 = 0$$

isentropic process

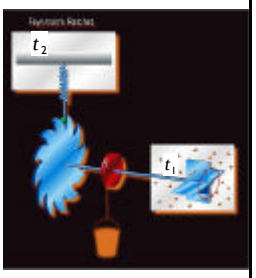

Ratchet Brownian motor

Angular velocity of ratchet: $\Omega = qn\left(f_B^f - f_B^b\right) = qn\left(e^{-\frac{e+Lq}{t_1}} - e^{-\frac{e}{t_2}}\right)$

Without load: $\Omega \xrightarrow{L=0} qn\left(e^{-\frac{e}{t_1}} - e^{-\frac{e}{t_2}}\right)$

Equal temperatures: $\Omega(L) \xrightarrow{t_1=t_2=t} qn\, e^{-\frac{e}{t}}\left(e^{-\frac{Lq}{t}} - 1\right)$

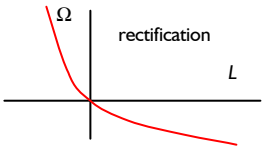

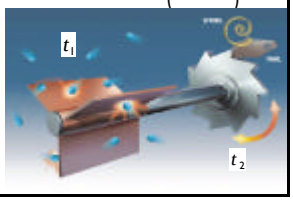

Escherichia coli ATP synthase

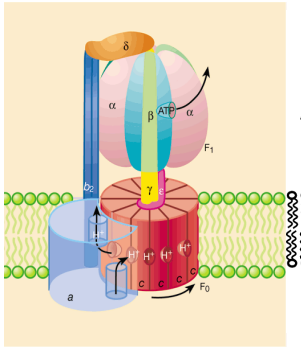

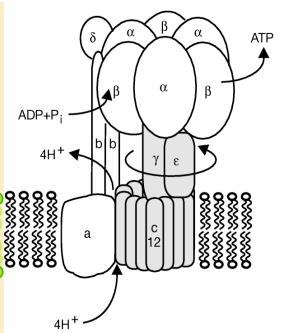

H. Wang and G. Oster (Nature 396:279-282 1998)

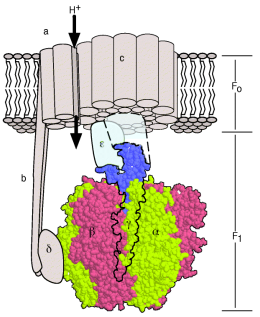

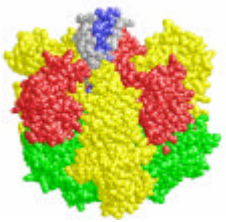

ATP synthase, H. Wang and G. Oster (Nature **396**, 279, 1998)

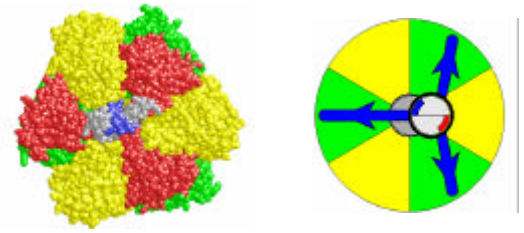

Myosin

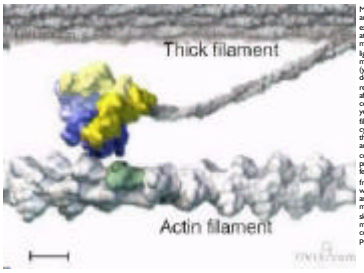

Muscle myosin is a dimerof two identical motor heads that are anchored to the thick filament (top) by a coiledcoil (gray rod extending to the upper right). The helicalactinfilament is shown at the bottom (gray). Myosin's catalytic core is blue and its mechanical elements (converter, lever arm helix and surrounding light chains) are colored yellow or red. In the beginning of the movie, the myosin heads are in the prestroke ADP·Pi state (yellow) and the catalytic cores bind weakly to actin . Once a head docks properly onto an actinsubunit (green), phosphate (Pi) is released from the active site. Phosphate release increases the affinity of the myosin head foractin and swings the converter/lever arm to the poststroke, ADP state (transition from yellow to red). The swing of the lever arm moves thactin filament by ~ 100 Å the exact distance may vary from cycle to cycle depending upon the initial prestroke binding configuration of the myosin onactin . After completing the stroke, ADP dissociates and ATP binds to the empty active site, which causes the catalytic core to detach from actin. The lever arm thenrecocks back to its prestroke state (transition from red to yellow). The surface features of the myosin head and the actin filament were rendered from Xray crystal structures by Graham Johnson (IIVth media: www.IIVth.com) using the programs MolView, Strata Studio Pro and Cinema 4D. PDB files used were ADP-AlF4-smooth muscle myosin (prestroke, yellow: #1BR2) and nucleotide-free chicken skeletal myosin (poststroke, red: #2MYS). Transitions between myosin crystal structure states were performed by computer coordinated extrapolations between the knownprestrokeand poststrokepositions.

http://www.sciencemag.org/feature/data/1049155.shl

Kinesin

The two heads of the kinesindimer work in a coordinated manner to move processivelyalong the microtubule. The catalytic core (blue) is bound to a tubulinheterodimer (green, b-subunit; white, asubunit) along a microtubule protofilament. (the cylindrical microtubule is composed of 13protofilament tracks). In solution, both kinesinheads contain ADP in the active site (ADP release is rateliminting in the absence of microtubules). The chaotic motion of the kinesinmolecule reflects Brownian motion. One kinesinhead makes an initial weak binding interaction with the microtubule and then rearranges to engage in a tight binding interaction. Only one kinesinhead can readily make this tight interaction with the microtubule, due to restrai nts imposed by the coiled -coil and pre-stroke conformation of the neck linker in the bound head. Microtubule binding releases ADP from the attached head. ATP then rapidly enters the empty nucleotide bind ing site, which triggers the neck linker to zipper onto the catalytic core (red to yellow transition). This action throws the detached head forward and allows it to reach the next tubulinbinding site, thereby creating a 2-head -bound intermediate in which the neck linkers in the trailing and leading heads are pointing forward (post-stroke, yellow) and backwards (pre-stroke; red) respectively. The trailing head hydrolyses the ATP (yellow flash of ADP -Pi), and reverts to a weak microtubule binding state (indicated by the bouncing motion) and releases phosphate (fading Pi). Phosphate release also causes the unzippering of the neck linker (yellow to red transition). The exact timing of the strongto-weak microtubule binding transition and the phosphate release step are not well-defined from current experimental data. During the time when the trailing head execut es the previously described actions, the leading head releases ADP, binds ATP, and zippers its neck linker onto the catalytic core. This neck linker motion throws the trailing head forward by 160 Å to the vicinity of new tubulinbinding site. After a random diffusional search, the new lead head docks tightly onto the binding site which comp letes the 80 Å step of the motor. The movie shows two such 80 Å steps of the kinesinmotor. The surface features of the kinesin motor domains and the microtubule protofilament were rendered from X -ray and EM crystallographic structures by Graham Johnson (IIVth media: www.IIVth.com) using the programs MolView, Strata Studio Pro and Cinema 4D. PDB files used were human conventional kinesin (prestroke red: # 1BG2) and rat conventional kinesin(poststroke yellow: #2KIN). In human conventional kinesin the neck linker is mobile and its located in the prestrokestate is estimated from cryo-electron microscopy data. Transitions between states were performed by performing computer-coordinated extrapolations between the prestrokeand poststroke positions. The durations of the events in this sequence were optimized for clarity and do not necessarily reflect the precise timing of events in the ATPcycle.

Molecular gears

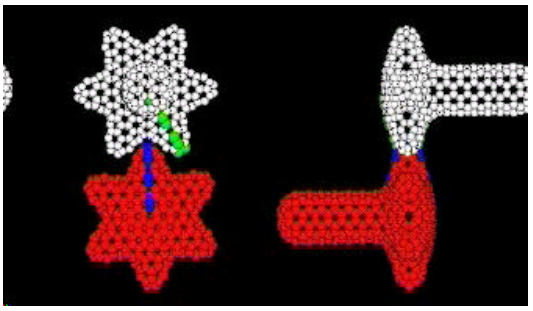

http://chem.iupui.edu/Research/Robertson/Robertson.html#Gears

Diffusion in asymmetric potentials

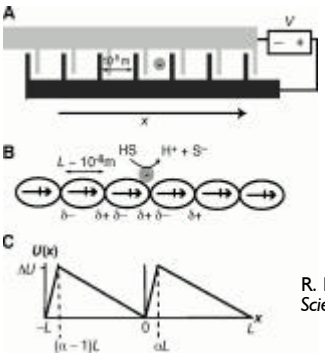

electrostatic potential

chemical potential

R. Dean Astumian, *Science* 1997 **276**: 917-922.

Driven Brownian ratchets

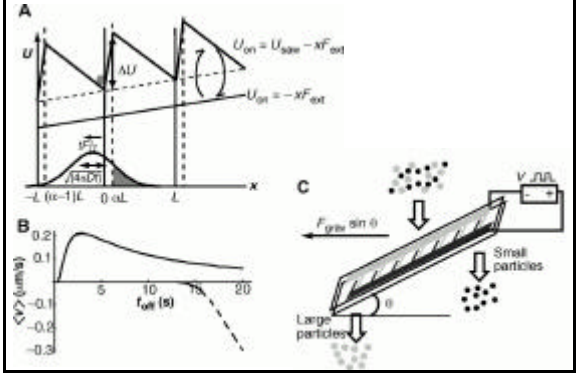

DNA transport by a micromachined Brownian ratchet device

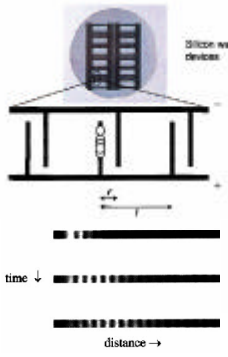

Joel S. Bader *et al.*, PNAS **96.** 13165 (1999)

Fig. 3. Three images are shown from a typical experiment using a device with 2-μm electrodes and a 0.7-Hz switching frequency to transport a rhodamine-labeled DNA 50-mer. These images were saved during the trapping phase of the cycle, and fluorescence maxima are clearly seen from DNA molecules captured on the positive electrodes. At the start of the experiment, the DNA oligomers are focused on left-most three electrodes. As the potential cycles between on- and off-states, the packet moves to the right and broadens.

Geometrical Brownian ratchet I

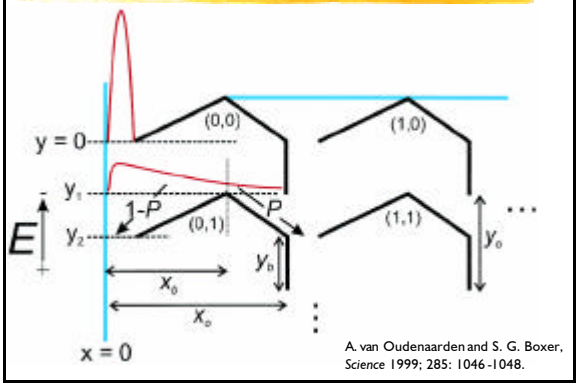

A. van Oudenaarden and S. G. Boxer, *Science* 1999; 285: 1046-1048.

Geometrical Brownian ratchet II

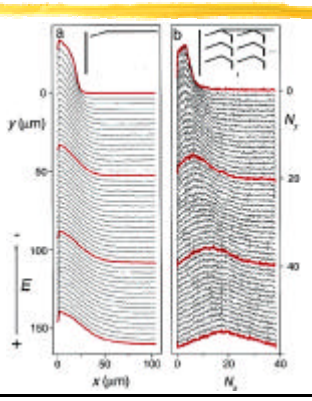

Unidirectional molecular rotation

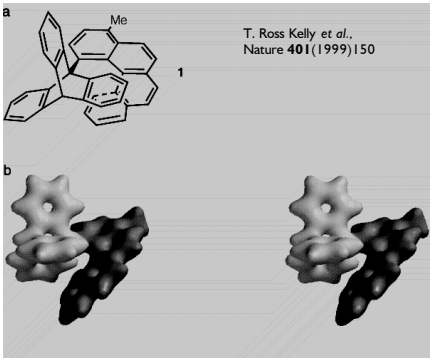

T. Ross Kelly *et al.*, Nature **401**(1999)150

Chemically driven rotation

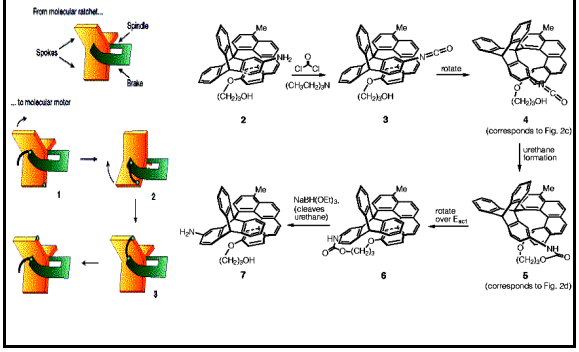

Light driven rotation

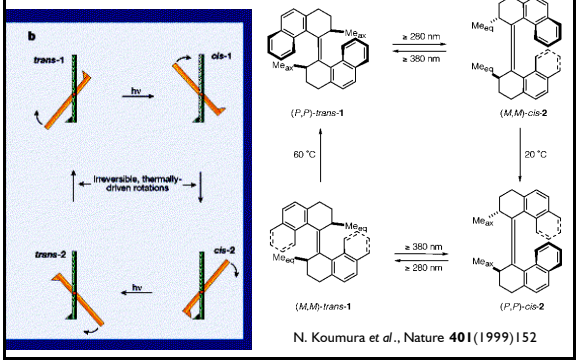

N. Koumura *et al.*, Nature **401**(1999)152

Maxwell's demon

W. Smoluchowski (1941):
No automatic, permanently effective perpetual motion machine van violate the second law by taking advantage of statistical fluctuations (Feynman: the demon is getting hot). Such device might perhaps function if operated by intelligent beings.

W.H. Zurek, Nature **341**(1989)119:
The second law is safe from intelligent beings as long as their abilities to process information are subject to the same laws as these of universal Turing machines.

Quantum demon? (ask Milena Grifoni)

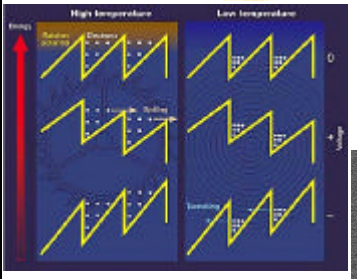

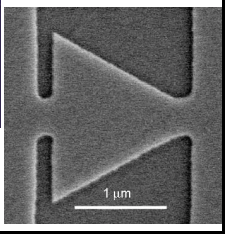

Fluctuations of μm-sized trapped colloidal particles

G.M. Wang *et al.*, Phys. Rev. Lett. 89(2002)050601

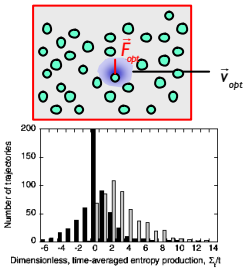

FIG. 1 (color online). Histogram of the dimensionless, time-averaged entropy production, Σ_t/t, from 540 experimental trajectories of a colloidal particle in an optical trap at times $t = 10^{-2}$ (black bars) and $t = 2.0$ (gray bars) seconds after initiation of stage translation. The bin size is $\Delta\Sigma_t/t = 1.0$.

physics.okstate.edu/
ackerson/vackerson/

$$\Sigma_t = \frac{1}{t}\int_0^t \vec{v}_{opt}\cdot\vec{F}_{opt}(s)\,ds$$

Entropy production